Effect of Low-Temperature Shock Compression on the Microstructure and Strength of Copper

DAVID H. LASSILA, TIEN SHEN, BU YANG CAO, and MARC A. MEYERS

Copper with two purities (99.8 and 99.995 pct) was subjected to shock compression from an initial temperature of 90 K. Shock compression was carried out by explosively accelerating flyer plates at velocities generating pressures between 27 and 77 GPa. The residual microstructure evolved from loose dislocation cells to mechanical twins and, at the 57 and 77 GPa pressures, to complete recrystallization, with a grain size larger than the initial one. The shock-compressed copper was mechanically tested in compression at a strain rate of 10^{-3} s^{-1} and temperature of 300 K; the conditions subjected to lower pressures (27 and 30 GPa) exhibited work softening, in contrast to the conventional work-hardening response. This work softening is due to the uniformly distributed dislocations and the formation of loose cells, evolving, upon plastic deformation at low strain rates, into well-defined cells, with a size of approximately 1 μm. The 99.995 pct copper subjected to the higher shock-compression pressures (57 and 77 GPa) exhibited a stress-strain response almost identical to the unshocked condition. This indicates that the residual temperature rise was sufficient to completely recrystallize the structure and eliminate the hardening due to shock compression. Thermodynamic calculations using the Hugoniot–Rankine conservation equations predict residual temperatures of 570 and 1000 K for the 57 and 77 GPa peak pressures, respectively.

I. INTRODUCTION

THIS contribution honors R.W. Armstrong and his seminal contributions to our understanding of the mechanical behavior of materials. Of great importance to the dynamic behavior of materials is the Zerilli–Armstrong equation, which has found application in computational simulations worldwide. It is anchored in the physical processes occurring in a material and has been instrumental in elucidating numerous phenomena. This is but one example of the broad contributions of R.W. Armstrong.

Shock-recovery experiments have been used to assess the effects of shock waves on the postshock microstructure and related mechanical behavior of copper and many other materials. These experiments are performed such that the imparted shock passes through the test material and is then dissipated in momentum traps. Shock-release waves from free surfaces in the momentum traps can prevent spurious plastic deformation from passing through the test material. This allows the test material to be recovered and then examined to assess only the effects of the passage of a uniaxial-strain shock-wave rise and release. Several types of loading (flyer-plate impact, laser-shock ablation, *etc.*) and momentum-trap arrangements have been employed.

In general, shock-recovery investigations performed on Cu and other fcc metals have shown that shock loading results in an increase in dislocation density, and general cellular dislocation structures are observed.[1,2,3] Deformation experiments performed on shock-recovered Cu over a wide range of conditions have shown "shock hardening" commensurate with the observed increase in dislocation density. For example, Gourdin and Lassila[4] showed that the postshock constitutive behavior of copper shocked to 10 GPa can be fitted using the mechanical threshold stress constitutive model by adjusting the value of the internal-state variables associated with dislocation density. Nevertheless, the work-hardening rate in shock-compressed samples was found to decrease with increasing peak pressure. Andrade and co-workers[5,6] observed a stress-strain curve that showed a very low work hardening after shock compression to a pressure of 50 GPa. Intriguing results obtained for shock-loaded nickel by Meyers[7] showed clear indication of work softening. This was interpreted as being due to the breakdown of the loose cellular structure upon quasistatic plastic deformation. Work softening had earlier been mentioned by Cottrell and Stokes[8] and was obtained by Longo and Reed Hill[9,10,11] when specimens were first deformed at 77 K and then at ambient temperature. Hammad and Nix[12] correlated dislocation densities with flow stress in Al and observed that dislocation reorganization leads to a decrease in work hardening; the extreme case would be work softening.

The temperature of a material as it is being shocked raises monotonically to a peak value (T_s) and then decreases when the shock release occurs. The temperature of the materials after the shock has passed is referred to as the residual shock temperature (T_r). Both T_s and T_r increase with the peak shock pressure. McQueen *et al.*[13] have predicted a temperature rise for a 300 K initial temperature. Figure 1 shows the calculated shock and residual temperatures as a function of peak shock pressure for both the 90 and 300 K initial temperatures. The shock temperatures were calculated using Eq. [5.44] from Meyers.[3] Since the heat capacity at 90 K (C_{v90}) is lower than the ambient-temperature value, C_{v300} (above which it is

DAVID H. LASSILA and TIEN SHEN, Research Scientists, are with the Lawrence Livermore National Laboratory, Livermore, CA 94550. BU YANG CAO, Graduate Student, and MARC A. MEYERS, Professor, are with the University of California, San Diego, La Jolla, CA 92093. Contact e-mail: bucao@ucsd.edu

This article is based on a presentation given in the symposium "Dynamic Deformation: Constitutive Modeling, Grain Size, and Other Effects: In Honor of Prof. Ronald W. Armstrong," March 2–6, 2003, at the 2003 TMS/ASM Annual Meeting, San Diego, California, under the auspices of the TMS/ASM Joint Mechanical Behavior of Materials Committee.

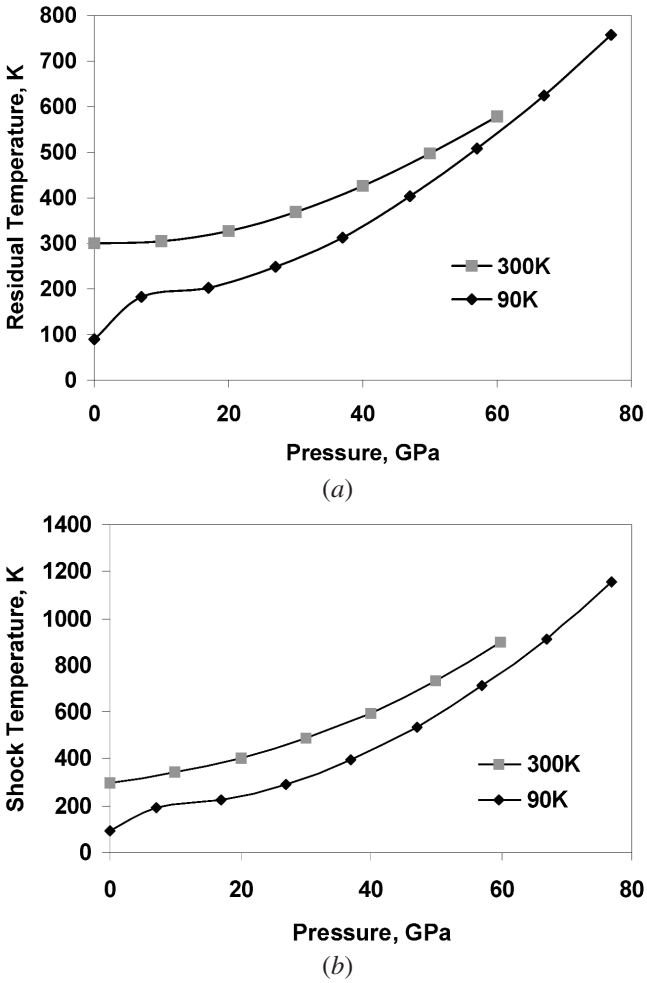

Fig. 1—Calculated (*a*) shock and (*b*) residual temperature for copper as a function of shock compression pressure with initial temperatures of 90 and 300 K.

constant), an average value of $(C_{v90} + C_{v300})/2$ was used for this interval. Above room temperature, the heat capacity was assumed to be constant. This provides a reasonable approximation to the shock temperature. The residual temperature was calculated by using Eq. [5.45] from Meyers.[3] The lower heat capacity in the temperature range of 90 to 300 K is reflected in the more rapid increase in the shock and residual temperatures in this domain, as seen in Figure 1.

The residual temperatures for the four pressures with an initial temperature of 90 K are

27 GPa: 248.5 K

30 GPa: 260 K

57 GPa: 508 K

77 GPa: 757 K

When performing shock-recovery experiments, it is imperative that the value of T_r, for a given cooling rate associated with the experimental setup, be less than the temperature that can promote static recovery and recrystallization in the study material. For this reason, the shock-recovery experiments have been designed to enhance the cooling rate by projecting the recovery assemblies into water-soaked catch materials.

The temperature (or thermal history), which promotes recrystallization and/or "recovery" of shock-induced internal dislocation structures, is very dependent on the microstructural state of the material (*i.e.*, stored elastic and defect energy associated with dislocation structures). For example, large amounts of mechanical work can substantially reduce the recrystallization temperature of Cu and other metals and alloys. Also, the chemical composition of Cu will affect recovery. Thus, both the shock conditions (T_r and shock-induced dislocations) and the chemical composition and impurity concentrations of the Cu can affect the "observed" shock effects in even the most carefully executed experiments. While these effects have been known, few experimental studies have been conducted to assess and/or quantify their effect on postshock microstructures and mechanical behavior.

We present the results of shock-recovery experiments performed on Cu at subambient temperature over a range of shock pressures. All of the experiments were performed at about 90 K, so that the values of T_r would be reduced relative to the values if the experiments were performed at room temperature. This was done in an attempt to mitigate static-recovery effects. The effect of impurity concentration was evaluated by performing experiments on two grades of commercially available Cu materials. The postshock microstructures were examined using optical metallography and transmission electron microscopy (TEM). Also, the effects of shock-induced microstructures on yield strength and work hardening were studied through the use of uniaxial-stress compression experiments.

II. EXPERIMENTS

A. *Shock-Recovery Experiments*

The shock-recovery experiments were performed by accelerating a flyer plate by an explosive charge, as shown schematically in Figure 2(a). Two unalloyed polycrystalline Cu conditions were used in this experiment: an oxygen flow electronic (OFE) Cu with a nominal purity of 99.8 pct and a high-purity (HP) Cu, which was determined to be 99.995 pct Cu. It should be noted that monocrystalline copper specimens were shock compressed in the same experiments and are being characterized as part of a continuing effort (not reported here). The momentum traps (spall and lateral) and anvil were made from a Cu-Be alloy known for its enhanced strength relative to unalloyed Cu. Several different methods were employed to attach the cover plate over the samples, including Cu rivets and brazing. However, the best technique was found to be electrodeposition of the Cu cover-plate material directly on the anvil/sample assembly, followed by finish machining to a high tolerance (prior to electrodeposition, the Cu samples were protected with a release agent).

The shock-recovery experiments were performed over a range of shock pressures and at low initial temperature by cooling the assembly with liquid nitrogen. The flyer-plate velocity was determined by using pins located in four positions equally spaced around the lateral-momentum trap (Figure 2(a)). The shock pressures were determined using the flyer-plate velocity in conjunction with the U_s-U_p Hugoniot.[15]

Four shock-recovery experiments were performed with peak pressures of 27, 30, 57, and 77 GPa and initial pulse duration of approximately 1 μs; the values of T_r were estimated to be 248.5, 260, 508, and 757 K for these shock pres-

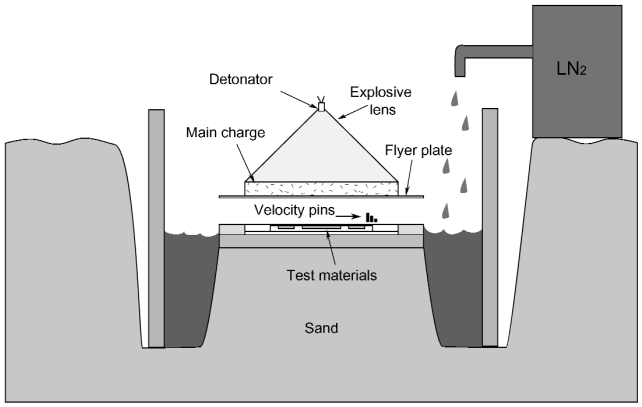

(*a*)

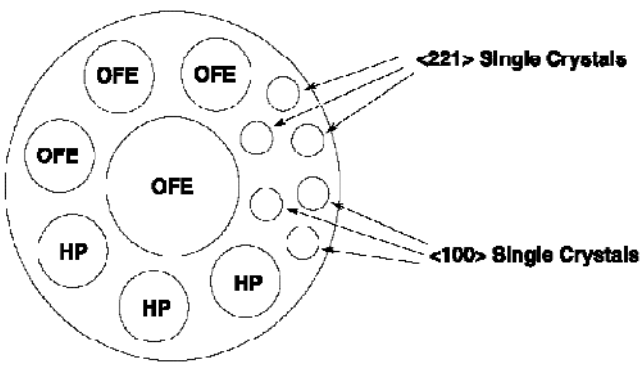

(*b*)

Fig. 2—(*a*) Schematic of shock recovery experiments performed by acceleration of a flyer plate by an explosive charge. (*b*) Anvil with OFE, HP, and single-crystal test samples (the postshock microstructures and mechanical behavior have not been studied).

sures, respectively (Figure 1). The planarity of the flyer-plate impact was assessed by analysis of the arrival times as determined by the various pin locations and was found to be acceptable for our experiment (within 10 deg). In general, the recovered test materials were found to be in good shape after the explosive loading; the flatness of the disks was found to be within 250 μm.

B. *Uniaxial-Stress Deformation Experiments*

The stress-strain response of the unshocked and shock-recovered materials was determined to evaluate the effects of shock hardening and also to correlate shock-hardening effects with shock-induced changes in the microstructure. Compression samples were manufactured from the shock-recovered disks using electrodischarge machining. Prior to testing, the ends of the samples were lapped parallel to within 10 μm. Uniaxial-compression deformation experiments were performed over a range of strain rates (10^{-3} s^{-1} to approximately 5000 s^{-1}), using a conventional screw-driven test machine for the low-strain-rate tests and a split Hopkinson pressure bar for the high-strain-rate experiments. The low-strain-rate experiments were performed using a high-precision subpress with an extensometer attached to the platens. The ends of specimens and platens were lubricated with molybdenum disulfide powder.

The stress-strain responses of the unshocked and shock-recovered materials are shown in Figure 3. There are at least

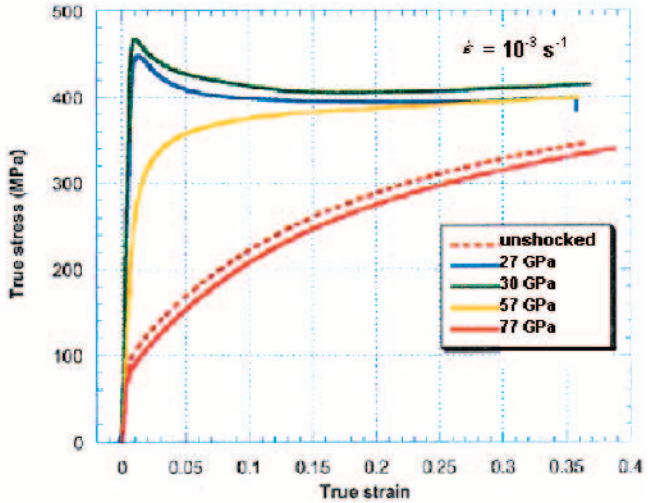

(*a*)

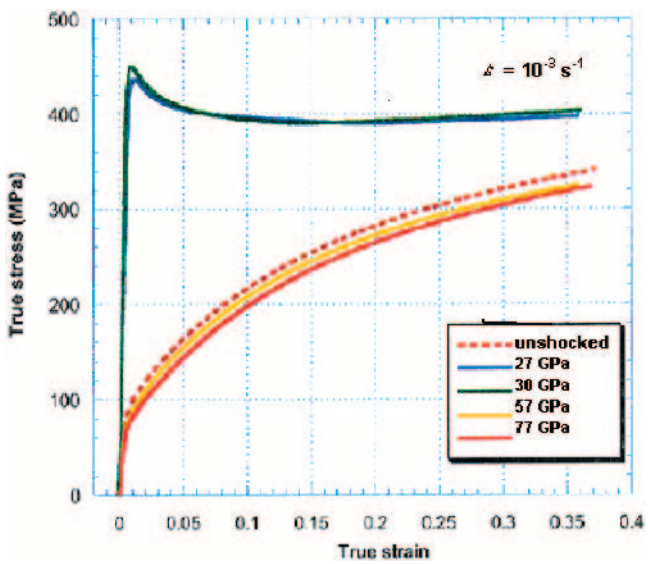

(*b*)

Fig. 3—Stress-strain curves of shock-recovered Cu samples under compression test: (*a*) OFE Cu tested at 300 K and (*b*) HP Cu tested at 300 K.

two major conclusions from looking at the data: first, extensive shock-hardening effects are seen in the specimens subjected to 27 and 30 GPa. In the high-pressure experiments (57 and 77 GPa), recovery is apparent. For the 99.995 pct Cu, the stress-strain curves are below the initial condition. This is consistent with the larger grain size observed after shock loading (Section II–C). For the 99.8 pct Cu, the stress-strain curve for the 57 GPa condition shows less hardening than the lower pressures. This can only be due to the recovery of the substructure, since it has undergone greater shock hardening at the higher pressure. The 57 GPa curve falls below the one for the unshocked condition, for the 99.9995 pct Cu. These results are consistent with the lower recrystallization temperature for this purity level.

The second notable finding is that some of the shock-recovered materials exhibit significant work softening in their stress-strain response, similar to that observed in shock-recovered nickel.[7] Figure 4 shows the results from shock-loaded nickel.

The shocked nickel (20 GPa) tested at ambient temperature undergoes work softening. It can be seen that the postshocked material tested at 77 K shows the conventional work hardening. Meyers *et al.*[16] also observed work softening in an Fe-34.5 pct Ni alloy shocked to a pressure of 7.5 GPa. The interpretation given by Meyers[7] was that the substructure generated by shock was closer to the low-temperature, low-strain rate deformation substructure. This natural work hardening occurs during low-temperature mechanical deformation. The shocked substructure underwent collapse when tested at ambient temperature. The TEM analysis carried out by Meyers *et al.*[17] confirmed the breakup of the loose dislocation cell structure after postshock deformation. It is important to note that the earlier results by Meyers were obtained in tension. This leaves open the question whether the work softening observed was truly due to microstructural reorganization or whether it was due to an early tensile instability (necking). The present results, in compression, show incontrovertibly that the microstructure is "softening." A discussion of these results and correlation with the observed shock-induced microstructural effects are given in Section II–D.

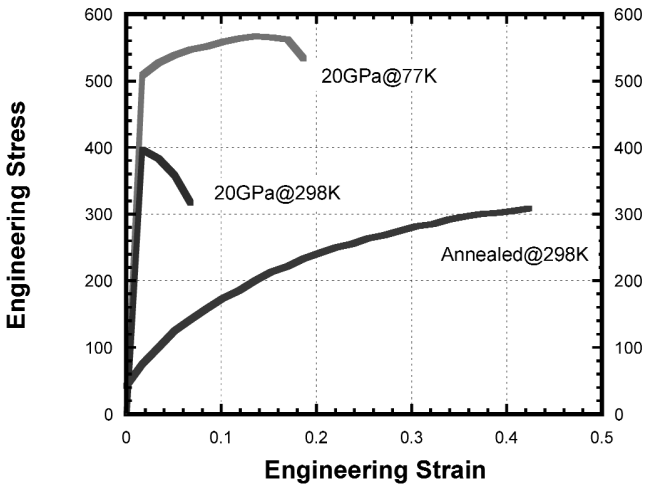

Fig. 4—Stress-strain curves for shock-recovered nickel samples under tension (adapted from Ref. 7).

Figure 5 shows the effect of temperature and strain rate on the stress-strain response of the shock-recovered Cu (30 GPa). Figure 5(a) refers to OFE copper, while Figure 5(c) refers to HP copper. The stress-strain response at 77 K shows the classical hardening behavior for the two cases, while the ambient-temperature response is characterized by a yield point followed by softening. A compression test carried out in a Hopkinson bar (strain rate of 5000 s^{-1}) reveals a situation intermediary between work softening and work hardening. The high strain

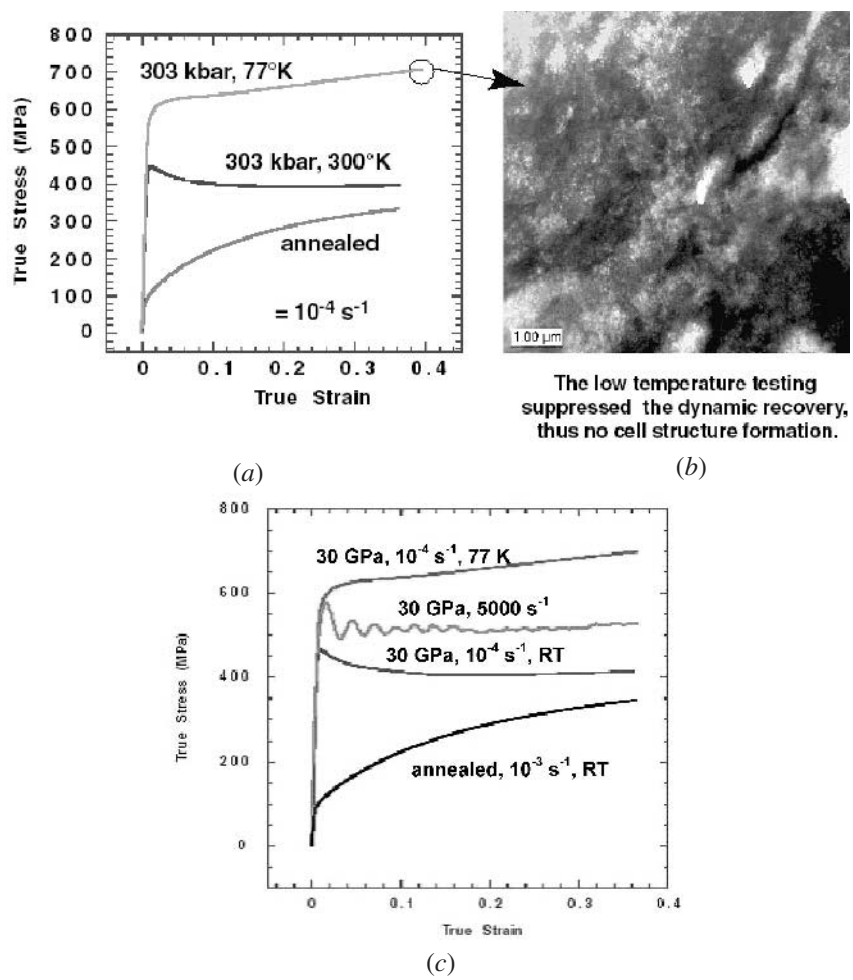

Fig. 5—Shock-recovered Cu samples under low-temperature compression test: (*a*) stress-strain curves of OFE, (*b*) TEM of Cu sample after 30 GPa and 77 K compression test, and (*c*) stress-strain curves of HP Cu.

rate at ambient teperature partially suppresses the dynamic recovery.

The results presented in Figure 5 are consistent with the early results by Meyers.[7] Figure 5(b) is the TEM micrograph for the OFE copper after being subjected to quasistatic compression; the dynamic recovery observed after ambient-temperature testing is suppressed. The fact that work softening was observed in compression testing is incontrovertible proof of this phenomenon.

C. *Microstructural Analyses*

Optical metallography was performed on the OFE and HP Cu in the unshocked and shock-recovered conditions. Samples were prepared by etching a polished surface normal to the shock-propagation direction with a solution of ammonium persulfate (20 pct) and water. Photographs of the etched surfaces are shown Figure 6. In the unshocked condition, the grain structure was found to be equal to grain sizes of 10 and 8 μm for the OFE

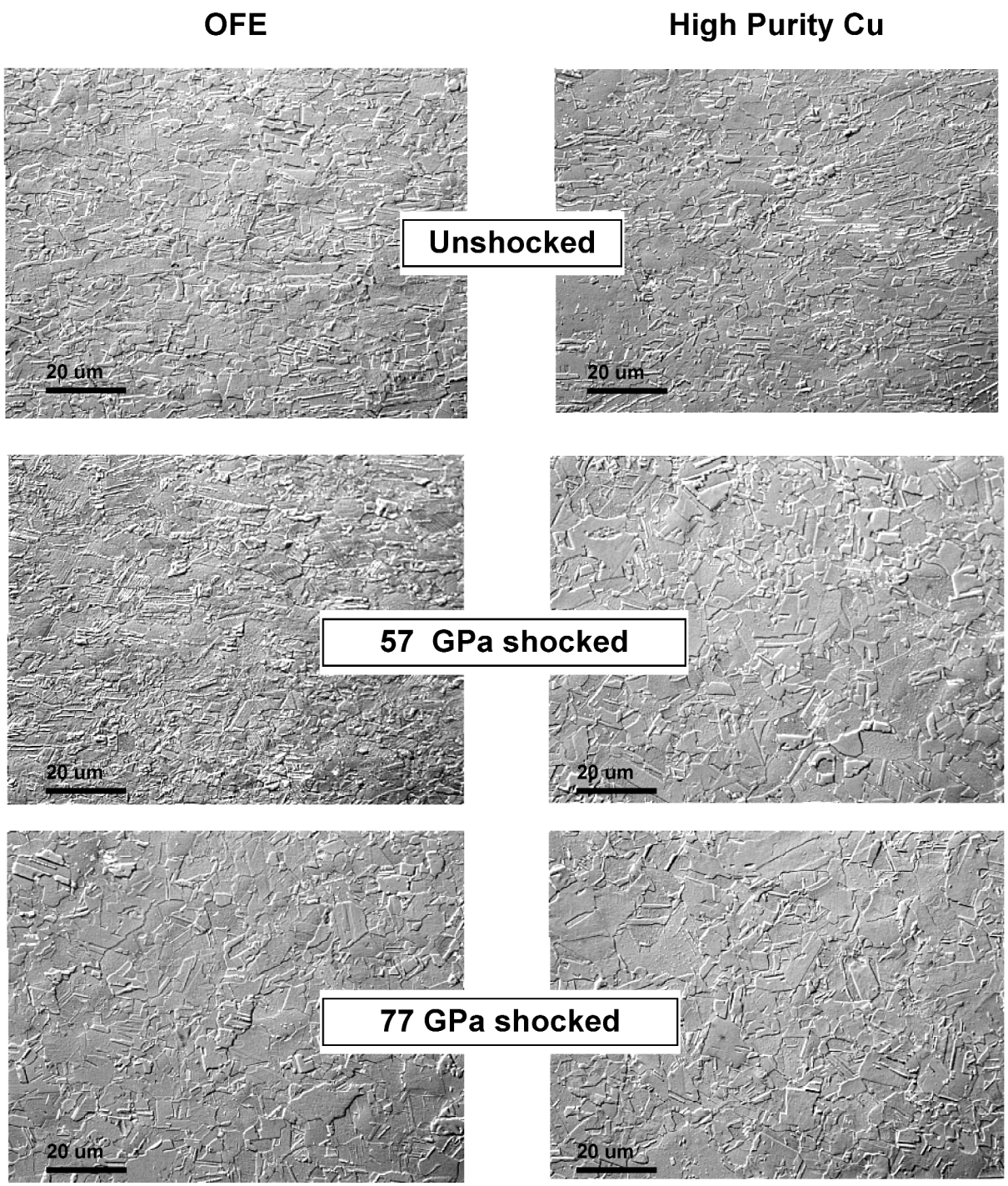

Fig. 6—Grain structures of OFE and HP Cu in unshocked and postshock conditions. In unshocked condition, both Cu samples contain annealing twins in grain structure. The amount of deformation twins increases (not shown) as shock pressure increases from 27 to 30 GPa. As the shocked pressure further increasd to 57 and 77 GPa, the Cu samples either slightly recovered (OFE) or fully recrystallized (HP). The 77 GPa postshock samples exhibit a larger grain size.

and HP materials, respectively. A standard line-intercept method was used for these grain-size determinations, and annealing twins were accounted for in the analysis.

In the shock-recovered condition, the microstructure of the OFE and HP Cu shocked to peak pressures of 27 and 30 GPa, respectively, exhibited significant amounts of what are believed to be shock-induced deformation twins (TEM analysis given in the following section confirmed this). Examples of twinned grains are marked by the arrows labeled as "A". A micrograph taken at a higher magnification, shown in Figure 7, shows the crystallographic nature of the deformation twins. We note here that not all of the grains showed deformation twins and, in particular, there appears to be an absence of twins in the larger grains (also shown in Figure 7). These grains are marked by the arrows labeled as "B". This is inconsistent with the results by Andrade *et al*.,[6] who observed a considerable grain-size dependence of mechanical twinning induced by shock loading, with large grains having a greater propensity for twin formation. Profuse twinning was observed after shock loading of 50 GPa for specimens with grain sizes of 117 to 315 μm. Specimens with grain size of 9.5 μm did not twin. It is, therefore, suggested that these large twin-free grains are the result of local recrystallization. In addition to deformation twins, many of the areas exhibited a "mottled" appearance suggestive of a highly dislocated structure. If, indeed, these grains are recrystallized, then the predicted residual temperature is underestimated. Section II–E addresses the possible contribution of frictional heat to this effect.

The OFE Cu shocked to a pressure of 57 GPa shows a similar structure to the materials shocked to 27 GPa and 30 GPa (*i.e*., significant amounts of deformation twins and dislocated structures). However, both the OFE and HP Cu shocked to a pressure of 77 GPa exhibited a recrystallized microstructure, and, in the case of the HP Cu, the grain size of the shock-recovered material was slightly increased relative to the unshocked material. This is a clear indication that the magnitude of T_r was significantly higher than the recrystallization temperature. Also, there appears to be a significant difference in the recrystallization temperature of the OFE *vs* that of the HP materials because, at the shock pressure of 57 GPa, the HP Cu was recrystallized, while, as indicated earlier, the OFE Cu was not.

Separate annealing experiments were carried out on HP copper shocked to 30.3 GPa at 393 K for durations between 3 and 600 minutes (Figure 8). The time corresponding to the onset in the drop of hardness (square symbols designate the average reading at each time) is approximately 20 minutes. Thus, the materials shocked to this pressure probably did not exhibit significant static recovery after shock loading, consistent with the mechanical-test data shown in Figure 3. Chojnowski and Cahn[14] determined the recrystallization temperatures for copper (OFE) shocked to 15.5 and 41 GPa. They obtained activation energies of 29 and 35.5 Kcal/mole, respectively. For the copper shocked at 41 GPa, they obtained a drop in mechanical properties (hardness and yield point) after a 15-minute anneal at 250 °C (523 K). Thus, this can be considered a safe estimate of the recrystallization temperature of copper shocked to this amplitude. The recrystallization temperature after the 15.5 GPa shock was higher: 400 °C (673 K).

D. *The TEM Characterization*

The effects of shock loading on the internal structure of the unshocked and shock-recovered materials were observed by TEM. A JEOL* 200CX microscope operating at 200 kV was used for the characterization. All images were recorded directly with a Gatan MultiScan close-coupled device camera. The TEM study focuses on the OFE Cu in the unshocked and shocked (30 GPa) conditions. Various samples were selected for TEM study based on our interest in the effects of strong shocks on the microstructure and also the effect of postshock deformation of the shock-induced microstructure.

*JEOL is a trademark of Japan Electron Optics Ltd., Tokyo.

1. *Unshocked OFE Cu*

The microstructure of unshocked OFE Cu contains a low density of dislocations and the typical {111} annealing twins. When this unshocked material was subjected to deformation in compression to 36 pct strain at 300 K and at a strain rate of 10^{-3} s^{-1}, the TEM microstructure showed the accumulation of glide dislocations and the development of $(1\bar{1}1)$ slip

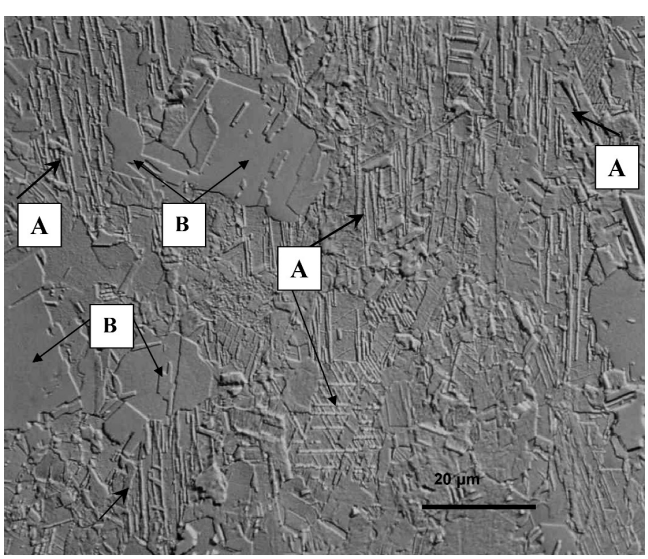

Fig. 7—Micrograph showing shock-induced deformation twins (OFE Cu, 27 GPa) (selected examples indicated by arrows A); regions that appear recrystallized are marked by arrows B.

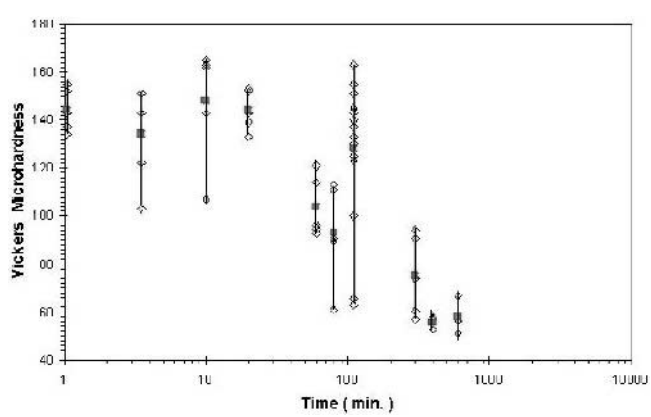

Fig. 8—Microhardness of HP Cu *vs* time at annealing temperature 393 K and shock pressure 30 GPa (average value: square).

bands. The {111} annealing-twin orientation was again identified by its diffraction pattern.

2. *Shock-Recovered OFE Cu (30 GPa)*

The shock-recovered OFE Cu was found to have a high density of forest dislocations (Figure 9(a)) and many fine deformation twins (Figure 9(b)). Also, fine elongated cell structures were observed (Figure 8(c)), reminiscent of transition bands. The thickness of these elongated cells was measured to be around 0.1 μm. This structure suggests that the dynamic recovery may have taken place in certain regions in the shocked OFE Cu sample due to adiabatic heating.

Quasistatic deformation (300 K, $\varepsilon = 0.37$) of the OFE Cu shocked to 30 GPa resulted in significant dislocation cell-structure development relative to the shock-induced substructure. As shown in Figure 10, distinct dislocation cell structures were observed, with an average cell diameter of approximately 1 μm in diameter. The scale of the cell is much larger than that observed in the postshock condition (0.1 μm). This microstructure reorganization produced by postshock quasistatic deformation has been observed previously by Meyers *et al.*[16] upon plastically deforming shock-loaded Ni. One with much larger cells replaced the shock-induced microstructure. As discussed previously, the stress-strain curve showed a work-softening phenomenon (an indication of dynamic recovery), which seems consistent with the evolution of a relatively uniform distribution of dislocations in the shock-recovered condition to a lower-energy cell structure during postshock quasistatic deformation.

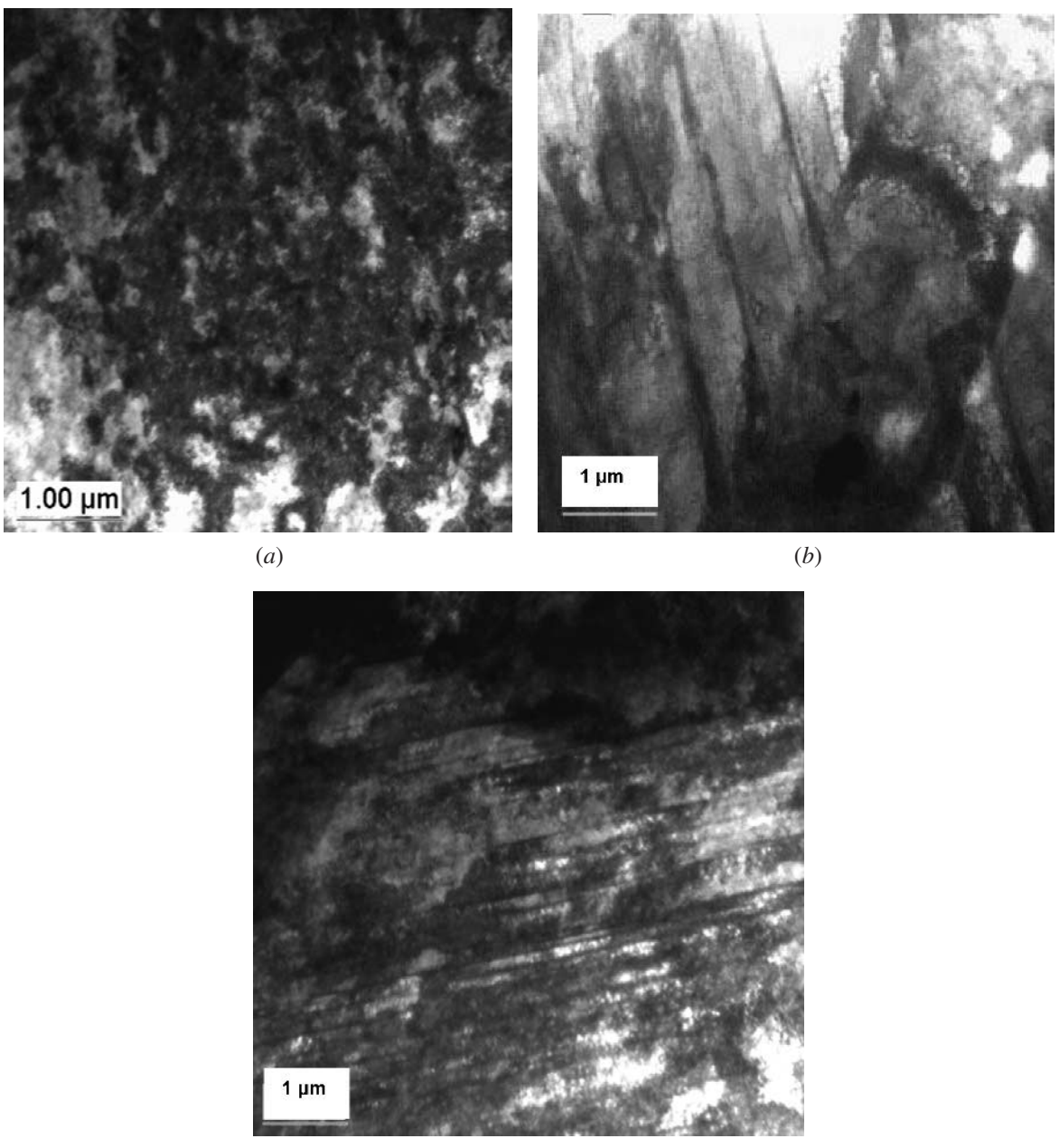

(*a*) (*b*)

(*c*)

Fig. 9—Three types of microstructure observed in OFE Cu sample shocked at 30 GPa: (*a*) high density of forest dislocations, (*b*) fine deformation twins, and (*c*) formation of transition-band-like fine elongated cell structure.

In contrast to the dislocation-structure evolution resulting from quasistatic deformation of shock-recovered 30 GPa Cu at 300 K, the same extent of quasistatic deformation at 77 K resulted in little change in the dislocation structure relative to the shock-recovered state. Instead, a further increase in the density of forest dislocations was observed with no significant cell evolution. This observation is consistent with the observed mechanical behavior shown in Figure 4 for nickel, in that the shock-recovered material was observed to have significant work hardening during the straining at 77 K. The results shown in Figure 5 for copper shock compressed to 30 GPa and tested at 77 K and 10^{-4} s^{-1} are in full agreement with the TEM observations. The shock-compressed copper work hardens; therefore, one would not expect a breakup of the dislocation substructure produced by shock compression. Clearly, the effects of thermal activation on the structure evolution of the shock-induced dislocation structure are important.

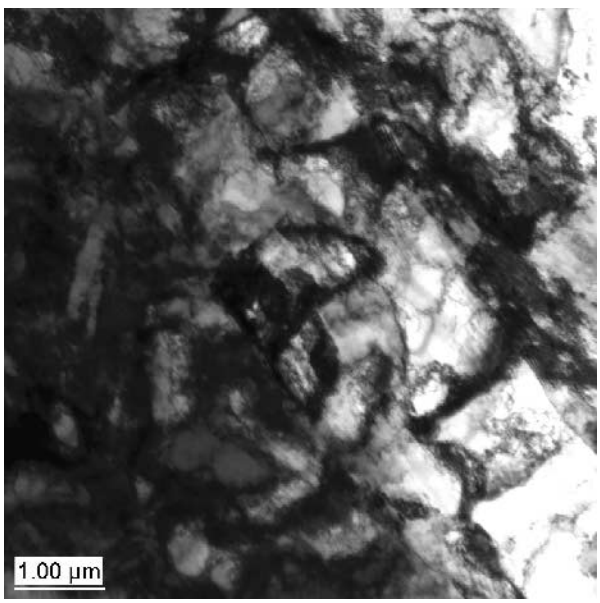

Fig. 10—Microstructure of 30 GPa postshock OFE Cu sample compression tested at 300 K to $\varepsilon = 0.37$ with $\dot{\varepsilon} = 10^{-3}$ s^{-1}.

E. *Characterization and Quantification of Shock-Induced Deformation Twins*

The metallographic examination of the OFE Cu shocked at 57 GPa suggested that this material developed extensive twinning within the grain structure. To obtain solid evidence of shock-induced deformation twinning, TEM analyses of microstructure of this material were performed. Figures 11 and 12 show the TEM bright- and dark-field images of deformation twins in OFE Cu shocked to 57 GPa. In Figure 11, the deformation twins were identified from the (011) diffraction pattern. By tilting the foil to align the twin plane closely parallel to the electron beam, the twin reflections in the diffraction

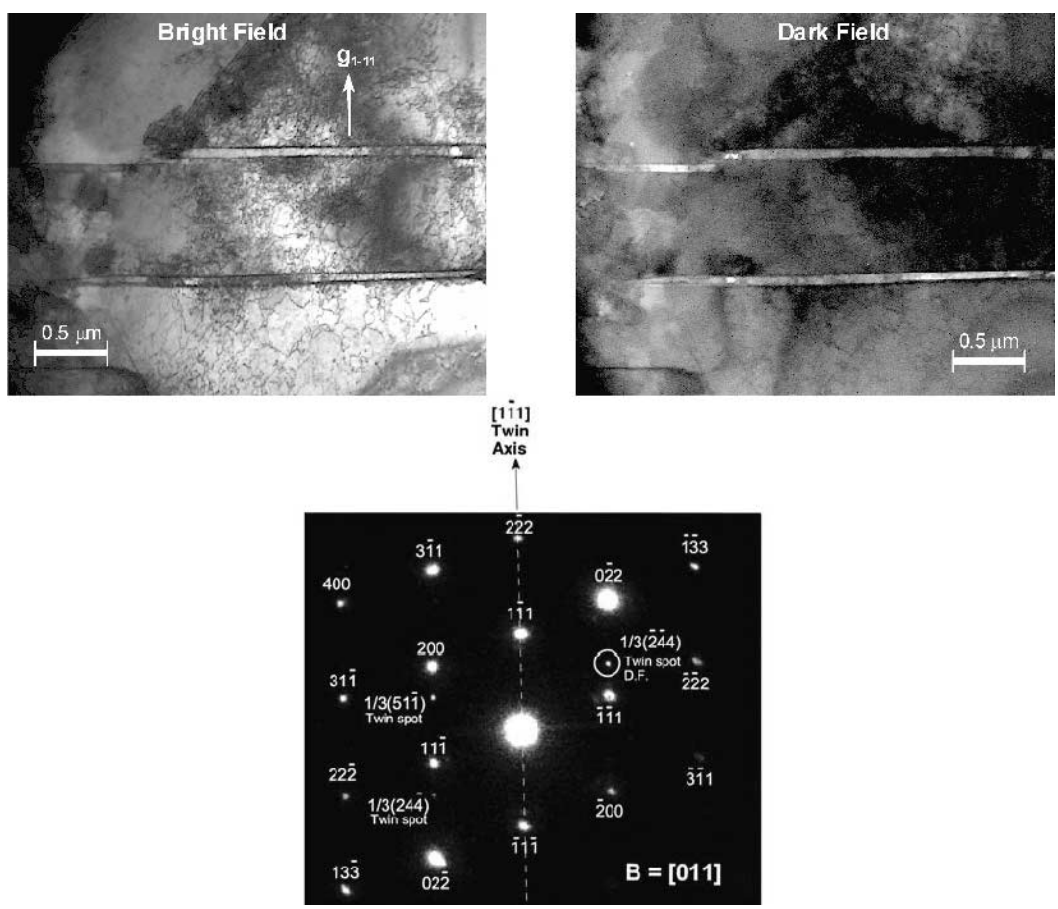

Fig. 11—OFE Cu shocked at 57 GPa showing the formation of (111) deformation twins as identified by (011) diffraction pattern.

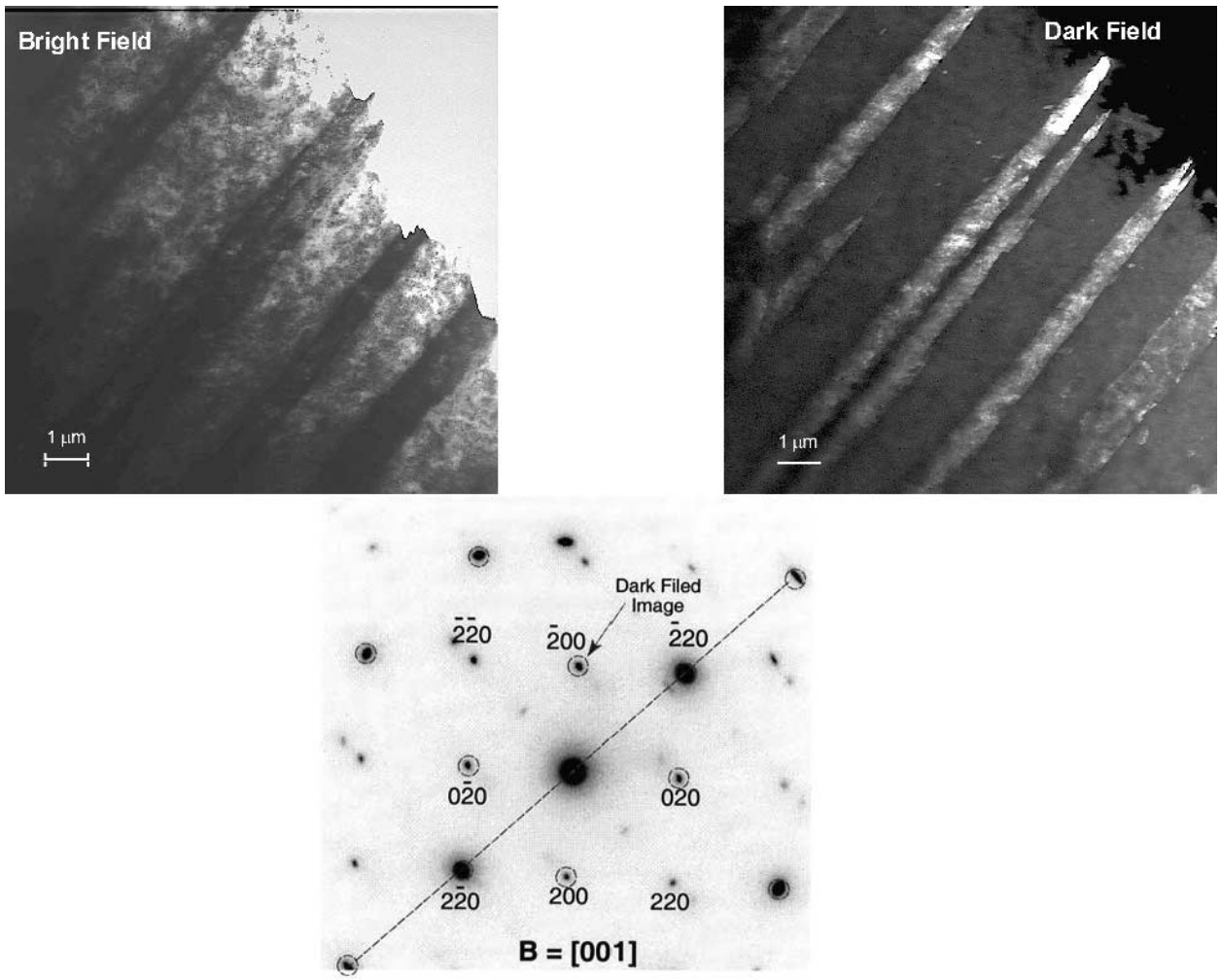

Fig. 12—OFE Cu shocked at 57 GPa showing the formation of (111) deformation twins as identified by (001) diffraction pattern.

pattern can be obtained and easily identified by a simple 180-deg rotation around the <111> twin axis. In the current case, the twin plane is $(1\bar{1}1)$ and the twin reflections are 1/3{244} and 1/3{511} as a result of twinning from the {200} and {111} planes, respectively. The dark-field image was taken from the 1/3 $(\bar{2}\bar{4}4)$ twin reflection.

Figure 12 shows deformation twins from the (001) diffraction pattern. The beam direction is not parallel with any twin plane, and twin reflections overlapped with the matrix diffraction spots. The dark-field image was taken from the 1/3 $(\bar{4}2\bar{4})$ twin reflection, which overlapped with the $(\bar{2}00)$ matrix reflection. Based on the TEM observation, the width of the deformation twins observed in the OFE Cu shocked at 57 GPa varied from 0.1 to 1 μm, and the occurrence of deformation twins varied from place to place.

Deformation-twin boundaries, which are similar in nature to annealing-twin boundaries, act essentially to refine the grain size of material. Zerilli and Armstrong[18] expressed the spacing of twin boundaries in terms of a Hall–Petch-type relationship and applied it to Armco iron. The incorporation of the strengthening due to twin boundaries into the Zerilli–Armstrong equation improved the match between predicted and experimentally observed deformation profiles in Taylor anvil specimens significantly. To estimate the possible "grain-refinement" effect of shock loading, we performed detailed metallography using Normarski interference contrast at a magnification of 500 times on samples that were etched in a solution of ammonium persulfate (20 pct) and water. A line-intercept method was used to determine the average number of intercepts, counting both high-angle grain boundaries and annealing and deformation twins. The data, summarized in Table I, indicate that the shock-recovered materials have a grain size approximately one-half that of the grain sizes in the unshocked condition, due to the presence of deformation twins. In other words, the effect of shock loading at pressures of about 30 GPa resulted in a grain-size refinement of about a factor of 2. As the pressure is increased at and above 57 GPa, this grain refinement disappears and is replaced by an increase in grain size. This is a direct result of recrystallization and is evident in Table I.

Table I. Effective Grain Sizes (in μm) of Unshocked and Shocked Cu (μm)

Materials	Unshocked	27 GPa	30 GPa	57 GPa	76 GPa
HP Cu	8	5	3	15	15
OFE Cu	10	2	5	5	15

F. *Additional Heating Term Due to Plastic Deformation*

It is instructive to estimate the effect of plastic deformation in the release portion of the wave on the residual temperature. The residual temperatures listed in Figure 1 are obtained from the shock temperature (T_s), assuming an isentropic release. This isentropic release is given by

$$T_r = T_s \exp\left[\frac{\gamma_0}{V_0}(V_s - V_0)\right] \quad [1]$$

where γ_0 is the Mie–Gruneisen parameter, V_0 is the initial specific volume, and V_s is the specific volume at the shocked state. In the case of the decompression of a solid with finite strength, one would need to add a heat component due to plastic deformation.

The temperature increase due to plastic deformation in the release portion of the wave can be expressed as

$$\Delta T_d = \frac{\beta}{\rho C_p}\int_{\varepsilon_0}^{\varepsilon_1} \sigma d\varepsilon \quad [2]$$

where ρ is the density, C_p is the heat capacity, and β is the Taylor factor. For the shock-compression case, the strain ε_1 is a function of V and V_0:

$$\varepsilon_1 = \frac{2}{3}\ln\frac{V_s}{V_0} \quad [3]$$

The strength of the material (σ) has to be estimated under the specified condition. This material has been shock hardened by the shock front that introduced a dense array of dislocations and/or twins. Zerilli and Armstrong[19,20] proposed a constitutive equation for incorporating the effects of strain, strain rate, and temperature. This Zerilli–Armstrong equation has the following form, for fcc metals:

$$\sigma = \sigma_G + kd^{-1/2} + B\exp(-\beta_0 T + \beta_1 T \ln\varepsilon) \quad [4]$$

The parameters obtained by Zerilli–Armstrong for copper are

$$\beta_0 = 0.0028\ \mathrm{K}^{-1}$$

$$\beta_1 = 0.000115\ \mathrm{K}^{-1}$$

$$B = 890\ \mathrm{MPa}$$

The term $\sigma_G + kd^{-1/2}$ incorporates all the athermal components of the flow stress. In our case, we approximate this term as 350 MPa. The strain rate at the release portion of the wave is on the order of 10^5 to $10^6\ \mathrm{s}^{-1}$. Substituting the previous parameters into the Zerilli–Armstrong equation [Eq. [4]) and assuming a perfectly plastic response ($n = 0$) and constant temperature ($T = 300$ K), we obtain

$$\sigma = 921.6\ \mathrm{MPa}\ (\dot{\varepsilon} = 10^5\ \mathrm{s}^{-1})$$

$$\sigma = 968.9\ \mathrm{MPa}\ (\dot{\varepsilon} = 10^6\ \mathrm{s}^{-1})$$

Applying an average value of $\sigma = 945.2$ MPa to Eq. [2], we obtain the increase in temperature due to plastic work. Figure 13 shows the temperature increase due to plastic deformation. This increase is modest and cannot account for differences in the recrystallization temperature observed. The experiments reported herein show a gap in pressure (the 30 to 57 GPa region). It would be necessary to carry out shock-compression experiments in this region to verify whether the residual temperature is, indeed, higher than the predictions from a simple isentropic release (without considering plastic dissipation processes in the release portion of the wave).

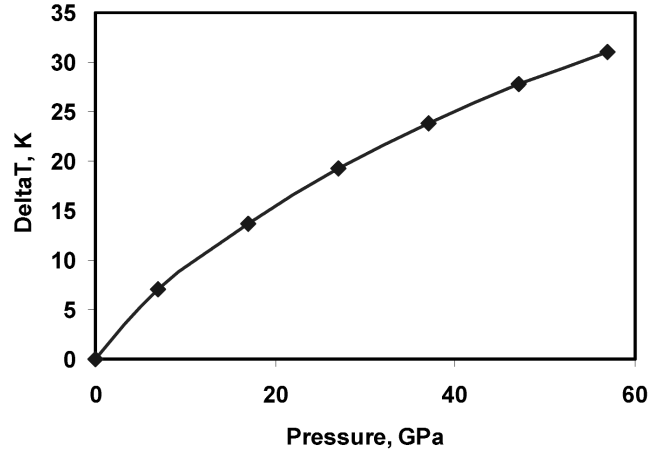

Fig. 13—Increase in residual temperature due to plastic deformation in the release portion of the wave.

III. SUMMARY AND CONCLUSIONS

Shock-recovery experiments were performed on OFE and HP Cu at subambient temperature (90 K) in an attempt to lower the postshock residual temperature and enable successful shock-recovery experiments at high pressures. The following is a summary of our findings.

1. Optical microscopy was performed to examine the effect of shock loading on the microstructure. Significant extents of deformation twinning (confirmed by TEM analyses) were observed in the shock-recovered materials that were not recrystallized. Our analyses suggest that the grain-size refinement due to shock loading at pressures of 27 and 30 GPa in the OFE and HP Cu materials is about a factor of 2.
2. Recrystallization occurred in the HP Cu after a 57 GPa shock; the expected residual shock temperature is 508 K. Also, we found that both OFE and HP Cu materials were fully recrystallized after recovery from a 77 GPa shock (expected residual temperature of 757 K). The residual temperature of the specimen is rapidly decreased due to postquenching of the fixture in water-soaked catch materials. Parallel recrystallization experiments carried out in the specimen subjected to 30 GPa shock (Figure 7) reveal a reduction in average microhardness number between 20 and 60 minutes for a temperature of 393 K. Chojnowski and Cahn[14] report a recrystallization temperature (15-minute anneal) of 573 K after a 40 GPa shock. Their copper (oxygen-free, high conductivity) is similar to OFE; both have a higher impurity level than our HP Cu.
3. Uniaxial stress-compression deformation experiments were performed to investigate the postshock mechanical behavior of the shock-recovered materials. Under deformation conditions where thermally activated processes are

minimal (*i.e.*, 77 K), the shocked and recovered material exhibited a gradual transition to plastic behavior and positive work hardening. However, the postshock mechanical behavior was found to be substantially different when testing was carried out at ambient temperature, showing a yield point, work softening, and almost no indication of positive work hardening out to a strain of 35 pct or more. This work softening had been detected earlier for shock-loaded Ni[7,17] and Fe-34 pct Ni.[16]

4. Transmission electron microscopy of shock-recovered OFE Cu (30 GPa) indicated that the shock-release process resulted in a fairly uniform dislocation structure. This is in contrast to dislocation cell structures observed in other shock-recovered copper materials, notably those shocked at ambient temperature. Upon subsequent quasistatic straining at room temperature, a cell structure evolved from the "uniform" structure to a cellular structure ($\sim$1 μm), and this correlated with the yield phenomena and work softening observed in the mechanical behavior.

ACKNOWLEDGMENTS

The authors thank Mr. Fred Sandstrom for assembly of the shock recovery experiments and for their execution. This was carried out at the Energetic Materials Research and Technology Center, New Mexico Institute of Mining and Technology. Also, we thank Robert P. Kershaw for performing the optical light metallographic examinations of the materials, and Mary M. LeBlanc and Scott Preuss for performing the mechanical testing of the shock/recovered materials. The help of Mr. Anuj Mishra with manuscript preparation is gratefully acknowledged.

REFERENCES

1. O. Johari and G. Thomas: *Acta Metall.*, 1964, vol. 12, pp. 1153-59.
2. R.L. Nolder and G. Thomas: *Acta Metall.*, 1964, vol. 12, pp. 227-40.
3. M.A. Meyers: *Dynamic Behavior of Materials*, John Wiley & Sons, Inc., New York, NY, 1994, pp. 382-447.
4. W.H. Gourdin and D.H. Lassila: *Mater. Sci. Eng. A*, 1992, vol. 151, pp. 11-18.
5. U.R. Andrade, M.A. Meyers, K.S. Vecchio, and A.H. Chokshi: *Acta Metall.*, 1994, vol. 42 (9), pp. 3183-195.
6. M.A. Meyers, U.R. Andrade, and A.H. Chokshi: *Metall. Mater. Trans. A*, 1995, vol. 26A, pp. 2881-93.
7. M.A. Meyers: *Metall. Mater. Trans. A*, 1977, vol. 8A, pp. 1581-83.
8. A.H. Cottrell and R.J. Stokes: *Proc. R. Soc. A*, 1955, vol. 233, pp. 17-34.
9. W.P. Longo and R.E. Reed Hill: *Scripta Metall.*, 1970, vol. 4, pp. 765-70.
10. W.P. Longo and R.E. Reed Hill: *Scripta Metall.*, 1972, vol. 6, pp. 833-36.
11. W.P. Longo and R.E. Reed Hill: *Metallography*, 1974, vol. 7, pp. 181-201.
12. F.H. Hammad and W.D. Nix: *Trans. ASM*, 1966, vol. 59, pp. 94-104.
13. R.G. McQueen, S.P. Marsh, J.M. Taylor, J.N. Frits, and W.J. Carter: in *High-Velocity Impact Phenomena*, R. Kinslow, ed., Academic Press, New York, NY, 1970, pp. 293-317.
14. E.A. Chojnowski and R.W. Cahn: in *Metallurgical Effects at High Strain Rates*, T.W. Rohde, B.M. Butcher, J.T. Holland, and C.H. Karnes, eds., Plenum, New York, NY, 1973, pp. 631-44.
15. *Shock Waves and High Strain Rate Phenomena in Metals*, M.A. Meyers and L.E. Murr, eds., Plenum Press, New York, NY, 1981.
16. M.A. Meyers, L.E. Murr, C.Y. Hsu, and G.A. Stone: *Mater. Sci. Eng.*, 1983, vol. 57, pp. 113-26.
17. M.A. Meyers, K.-C. Hsu, and K. Couch-Robino: *Mater. Sci. Eng.*, 1983, vol. 59, pp. 235-49.
18. F.J. Zerilli and R.W. Armstrong: in *Shock Waves in Condensed Matter*, S.C. Schmid and N.C. Holmes, eds., Elsevier Science Publishers B.V., Amsterdam, 1988, pp. 273-76.
19. F.J. Zerilli and R.W. Armstrong: *J. Appl. Phys.*, 1987, vol. 61, pp. 1816-25.
20. F.J. Zerilli and R.W. Armstrong: *J. Appl. Phys.*, 1990, vol. 68, pp. 1580-91.